DOI 10.1007/s11041-015-9807-4
Metal Science and Heat Treatment, Vol. 56, Nos. 11 – 12, March, 2015 (Russian Original Nos. 11 – 12, November – December, 2014)

UDC 669.018.58:536.45

HIGH-TEMPERATURE BEHAVIOR OF HARD MAGNETIC ALLOYS (R, Zr)(Co, Cu, Fe)$_z$ (R = Sm, Gd)

M. B. Lyakhova,[1] E. M. Semenova,[1] and R. P. Ivanov[1]

Translated from *Metallovedenie i Termicheskaya Obrabotka Metallov*, No. 11, pp. 27 – 33, November, 2014.

Hysteresis loops of cast specimens of $R_{0.85}Zr_{0.15}(Co_{0.70}Cu_{0.09}Fe_{0.21})_z$ (R = Sm, Gd) are measured in the temperature range of 20 – 600°C. The temperature dependences of their magnetic characteristics are plotted. The microstructure and the rearrangement of the domain structure in external fields are studied. It is shown that the specimens with a low stoichiometric ratio z, when most of the volume is occupied with a copper-enriched structural component with $z \sim 5 – 6$, exhibit the highest stability of the coercivity.

Key words: hard magnetic materials, magnetic hysteresis, coercivity, temperature stability, nanostructure, magnetic domain structure.

INTRODUCTION

Modern industry imposes strict requirements on the temperature stability of the magnetic properties and maximum operating temperature of permanent magnets. The most promising materials for high-temperature permanent magnets are cobalt-base alloys with additives of rare-earth metals (REM) possessing a high Curie temperature ($T_C > 800$°C). These alloys have served a base for developing multicomponent hard magnetic alloys of the Sm – Zr – Co – Cu – Fe system with high values of magnetic energy $(BH)_{max} = 280 – 320$ kJ/m^3 and coercivity $H_{cJ} > 2$ MA/m [1 – 3]. Such alloys have a heterogeneous "cellular" nanostructure that provides high hysteresis properties in the material and stability in a wide temperature range. It is possible to raise considerably the maximum operating temperature of such magnets. Today we know of Sm – Zr – Co – Cu – Fe alloys with an elevated content of copper. Despite the certain decrease in the saturation magnetization, the stability of the coercivity of these alloys is elevated markedly in a wide temperature range [4]. An individual group of alloys of the Sm – Zr – Co – Cu – Fe system exhibits elevated induction and magnetic flux upon growth in the temperature due to the ferromagnetic type of the ordering of the sublattices of gadolinium and cobalt [6, 7].

The aim of the present work was to analyze systematically the high-temperature behavior and structure of a wide group of (R, Zr)(Co, Cu, Fe)$_z$ alloys, where R is a rare-earth metal (samarium or gadolinium).

METHODS OF STUDY

We fabricated alloys of the R – Zr – Co – Cu – Fe system with a mass of 100 – 200 g by the method of high-frequency induction melting under excess argon pressure. Coarse-grained ingots were obtained by slow cooling of the melt at an average rate of 1 – 2 K/sec. Then we chipped individual grains 2 – 3 mm in diameter from the polycrystals for magnetic measurements and structural studies.

The specimens were heat treated in a mode optimum for obtaining high values of coercivity [7, 8], which involved homogenizing at 1170 – 1185°C for 3 h, quenching to room temperature, isothermal annealing at 800°C for 20 h, slow cooling to 400°C at an average rate of 2 K/min, and arbitrary cooling.

The microstructure and the domain structure were studied using Neophot-30 and Axiovert 200 MAT metallographic microscopes. The microstructure was uncovered by chemical etching; the domain structure was determined with the help of the Kerr polar effect.

The nanostructure of the alloys was studied with the help of a SOLVER P47 scanning probe microscope using contact scanning of the surface in the mode of measuring the lateral component of the force of interaction between the specimen and the probe. To determine the surface texture the specimens were subjected to electrochemical etching.

[1] Tver State University, Tver, Russia (e-mail: Lahova_M_B@mail.ru).

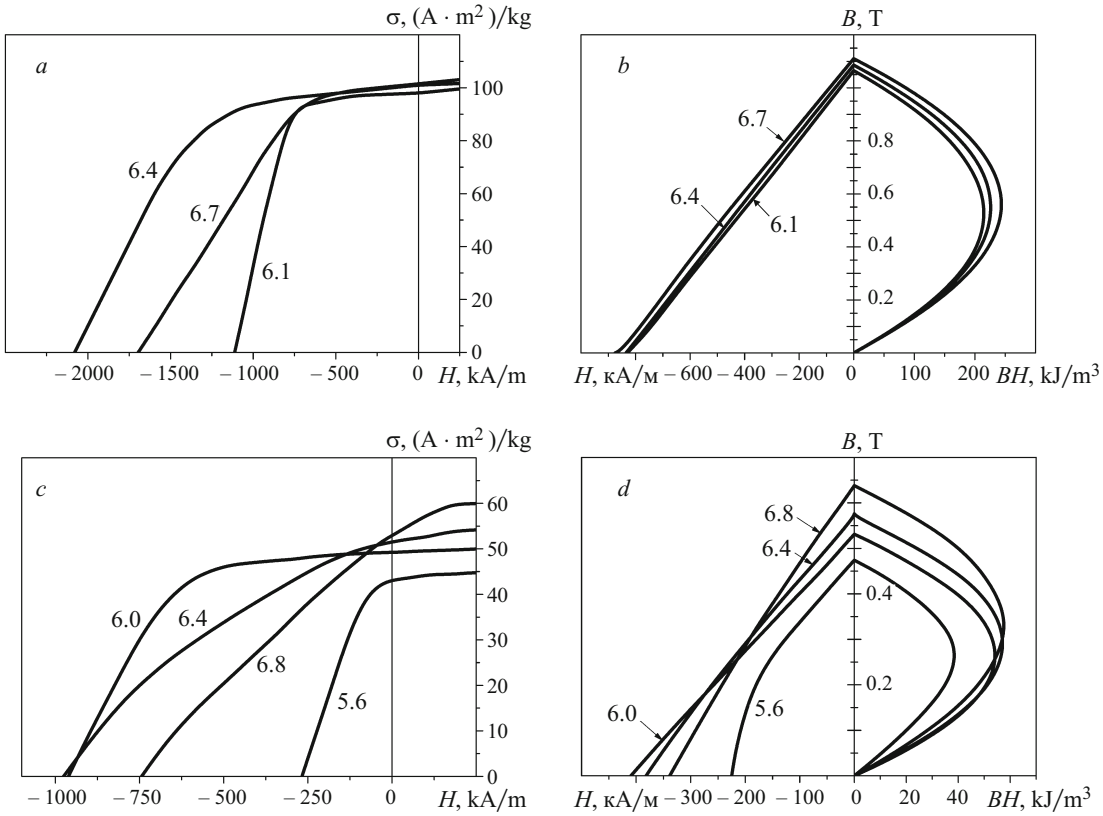

Fig. 1. Demagnetization parts of the hysteresis loops of σ(H) and B (H) and curves of energy product BH (B) of specimens of $R_{0.85}Zr_{0.15}(Co_{0.70}Cu_{0.09}Fe_{0.21})_z$ at 20°C (the values of z are given at the curves): *a*, *b*) R = Sm (a light REM); *c*, *d*) R = Gd (a heavy REM).

The specimens were magnetized in pulsed magnetic fields with intensity up to 8 MA/m in the solenoid of a capacitor pulse device. The magnetic measurements were performed in an open magnetic circuit by the method of vibration magnetometer. The magnetometer allowed us to measure the magnetic characteristics of the alloys on spheres 2 – 3 mm in diameter having a mass of 80 ± 40 mg. A temperature attachment to the magnetometer allowed us to perform the measurements at a temperature ranging from 20 to 600°C. The source of a constant magnetic field was an electromagnet with maximum field of ± 2 MA/m in the operating clearance of 30 mm.

RESULTS AND DISCUSSION

We chose two groups of alloys for the investigation, namely,

(*1*) $Sm_{0.85}Zr_{0.15}(Co_{0.70}Cu_{0.09}Fe_{0.21})_z$, where z = 6.1, 6.4 and 6.7;

(*2*) $Gd_{0.85}Zr_{0.15}(Co_{0.70}Cu_{0.09}Fe_{0.21})_z$, where z = 5.6, 6.0, 6.2, 6.4 and 6.8.

The alloys of the first group alloyed with Sm (a light REM) are ferromagnetics and exhibit high magnetization, coercivity and maximum energy product. These alloys are used widely as materials for high-energy-intensity permanent magnets.

The alloys of the second group with Gd (a heavy REM) possess ferromagnetic ordering and are magnetic materials with positive temperature coefficient of induction.

Temperature Dependences of Magnetic Characteristics of Alloys $R_{0.85}Zr_{0.15}(Co_{0.70}Cu_{0.09}Fe_{0.21})_z$

We measured hysteresis loops for all the $R_{0.85}Zr_{0.15}(Co_{0.70}Cu_{0.09}Fe_{0.21})_z$ alloys at different temperatures ranging from 20 to 600°C. As an example, we present in Fig. 1*a* and *c* the demagnetization parts of the hysteresis loops of the alloys with Sm and Gd at 20°C. In both groups the growth in z is accompanied by increase in the saturation magnetization, but at very high z (z = 6.7 for R = Sm and z = 6.4 and 6.8 for R = Gd) the rectangularity of the hysteresis loops worsens noticeably. By the data of [2, 5] the value of H_{cI} is the highest at medium z (z = 6.4 for R = Sm and z = 6.2 for R = Gd); such alloys contain equal volumes of the main structural components.

We plotted the demagnetization parts of the hysteresis loops in coordinates "magnetic induction B – true magnetic field H" for all the $R_{0.85}Zr_{0.15}(Co_{0.70}Cu_{0.09}Fe_{0.21})_z$ alloys and the curves of the energy product BH (B), which were used to

determine the value of the maximum energy product $(BH)_{max}$ (Fig. 1*a* and *b*).

The loops of $B(H)$ for the alloys of the first group at 20°C are virtually linear (Fig. 1*b*). In the alloys of the second group linearity of the $B(H)$ loops is typical for the specimens with $z = 5.6$ and 6.0 (Fig. 1*d*). It should be noted that the hysteresis loops for all these specimens remain rectilinear until 200 – 250°C.

We used the data measured for the two groups to plot the temperature dependences of the hysteresis characteristics (Figs. 2 and 3). For the $Sm_{0.85}Zr_{0.15}(Co_{0.70}Cu_{0.09}Fe_{0.21})_z$ alloys (Fig. 2*a*) the temperature dependences of the specific saturation magnetization σ_s have a ferromagnetic drooping nature. The highest fall of σ_s upon growth of the temperature is observed for the alloy with $z = 6.7$, which is connected with the higher content of iron and cobalt in the latter. The specific residual magnetization σ_r (Fig. 2*b*) and the residual induction B_r (Fig. 2*g*) also decrease monotonically upon growth of the temperature for all the alloys.

The coercivity H_{cI} of all the $Sm_{0.85}Zr_{0.15}(Co_{0.70}Cu_{0.09}Fe_{0.21})_z$ alloys decreases with growth of the temperature (Fig. 2*c*). The reduced temperature dependences $H_{cI}/H_0(t)$ (Fig. 2*d*) show that the temperature stability of H_{cI} lowers upon growth of z. For example, at 300°C the value of H_{cI} decreases by 27, 44, and 68% for the specimens with $z = 6.1$, 6.4 and 6.7, respectively (Fig. 2*d*).

It can be seen from Fig. 2*d* that in all the specimens of $Sm_{0.85}Zr_{0.15}(Co_{0.70}Cu_{0.09}Fe_{0.21})_z$ growth of the temperature is accompanied by decrease of the induction coercivity H_{cB} too. The temperature dependences of the reduced coercivity H_{cB}/H_0 (Fig. 2*f*) show that the specimen with the highest $z = 6.7$ has the lowest stability of H_{cB}. For the specimens with $z = 6.1$ and 6.4 the curves of $H_{cB}/H_0(t)$ behave similarly in the temperature range of 20 – 400°C.

For all the specimens of $Sm_{0.85}Zr_{0.15}(Co_{0.70}Cu_{0.09}Fe_{0.21})_z$ the maximum energy product decreases monotonically upon growth of the temperature (Fig. 2*h*). The specimens with $z = 6.1$ and 6.4 are characterized by a comparatively higher stability of $(BH)_{max}$ than the specimen with $z = 6.7$.

The temperature dependences of the hysteresis characteristics of alloys $Gd_{0.85}Zr_{0.15}(Co_{0.70}Cu_{0.09}Fe_{0.21})_z$ are presented in Fig. 3. It can be seen that the curves of the specific saturation magnetization $\sigma_s(t)$ are typical for ferromagnetics. The value of σ_s increases with growth of the temperature from room one to 250 – 300°C (Fig. 3*a*).

The dependences of the specific residual magnetization $\sigma_r(t)$ and residual induction $B_r(t)$ differ noticeably from $\sigma_s(t)$, especially for the specimens of $Gd_{0.85}Zr_{0.15}(Co_{0.70}Cu_{0.09}Fe_{0.21})_z$ with $z = 6.4$ and 6.8 and low rectangularity of the hysteresis loops (Fig. 3*a*, *b*, and *g*). The magnetization coercivity H_{cI} of the specimens of the second group (with cadmium) decreases monotonically with growth of the temperature. However, analysis of the temperature dependences of the reduced coercivity $H_{cI}/H_0(t)$ shows two things, i.e., (*1*), just as for the specimens with samarium, the stability of H_{cI} of the specimens of $Gd_{0.85}Zr_{0.15}(Co_{0.70}Cu_{0.09}Fe_{0.21})_z$ worsens upon growth of the value of z and (*2*) the behavior of the curves of $H_{cI}/H_0(t)$ is virtually the same both for the specimens with $z = 6.4$ and for the specimens with $z = 6.8$ (Fig. 3*d*).

Analyzing the temperature dependences of the induction coercivity H_{cB} and its reduced values H_{cB}/H_0 (Fig. 3*e* and *f*) we discovered a new feature of alloys $Gd_{0.85}Zr_{0.15}(Co_{0.70}Cu_{0.09}Fe_{0.21})_z$. For the specimen with $z = 6.0$ the value of H_{cB} increased by about 7% when the temperature grew from room one to 150°C. This increase in H_{cB} is connected with the ferromagnetic nature of the temperature dependences of the magnetization and with the preserved high rectangularity of the hysteresis loops of this specimen in the temperature range considered.

The same factors also explain the growth of the maximum energy product $(BH)_{max}$ of the specimens of $Gd_{0.85}Zr_{0.15}(Co_{0.70}Cu_{0.09}Fe_{0.21})_z$ with $z = 5.6$, 6.0 and 6.4 upon growth of the temperature (Fig. 3*h*). For example, the value of $(BH)_{max}$ of the specimen with $z = 6.0$ increased from 55 kJ/m^3 at 20°C to 69 kJ/m^3 at 250°C.

Microstructure and Domain Structure of Alloys $R_{0.85}Zr_{0.15}(Co_{0.70}Cu_{0.09}Fe_{0.21})_z$

Light microscopy of alloys (R, Zr)(Co, Cu, Fe)$_z$ with samarium and gadolinium shows that they contain three structural components (see Fig. 4*a*) denoted conventionally *A* (the dark regions), *B* (the gray regions), and *C* (the white regions) [2, 5]. Thin plates of component C are always located inside component A and oriented in parallel to the base plane of the specimens.

The chemical analysis of the structural components performed in [2, 3] has shown that component *A* has stoichiometric ratio $z \sim 5 – 6$ and is enriched with copper relative to the average composition of the alloy. Component *B* ($z \sim 7 – 7.5$) is enriched with iron, and component *C* has a high concentration of zirconium.

The studies of [9] performed by the methods of atomic-force microscopy (AFM) on etched surfaces of specimens of (R, Zr)(Co, Cu, Fe)$_z$ have shown that the configuration of component *B* is very close to the "cellular" structure of permanent magnets [10], and component *A* contains rounded precipitates (Fig. 5). Such configuration of the nanostructure of components *A* and *B* is an evidence in favor of the model of structure formation suggested for the materials in question in [3].

We studied the domain structure and the processes of its rearrangement in external demagnetizing fields for specimens of the second group (with cadmium).

Figure 4 presents photographs of the microstructure and domain structure in the same regions of the base plane of specimens of $Gd_{0.85}Zr_{0.15}(Co_{0.70}Cu_{0.09}Fe_{0.21})_z$ with $z = 5.6$, 6.0, 6.4 and 6.8. The configuration of the domain structure of each specimen corresponds to the state after the action of a

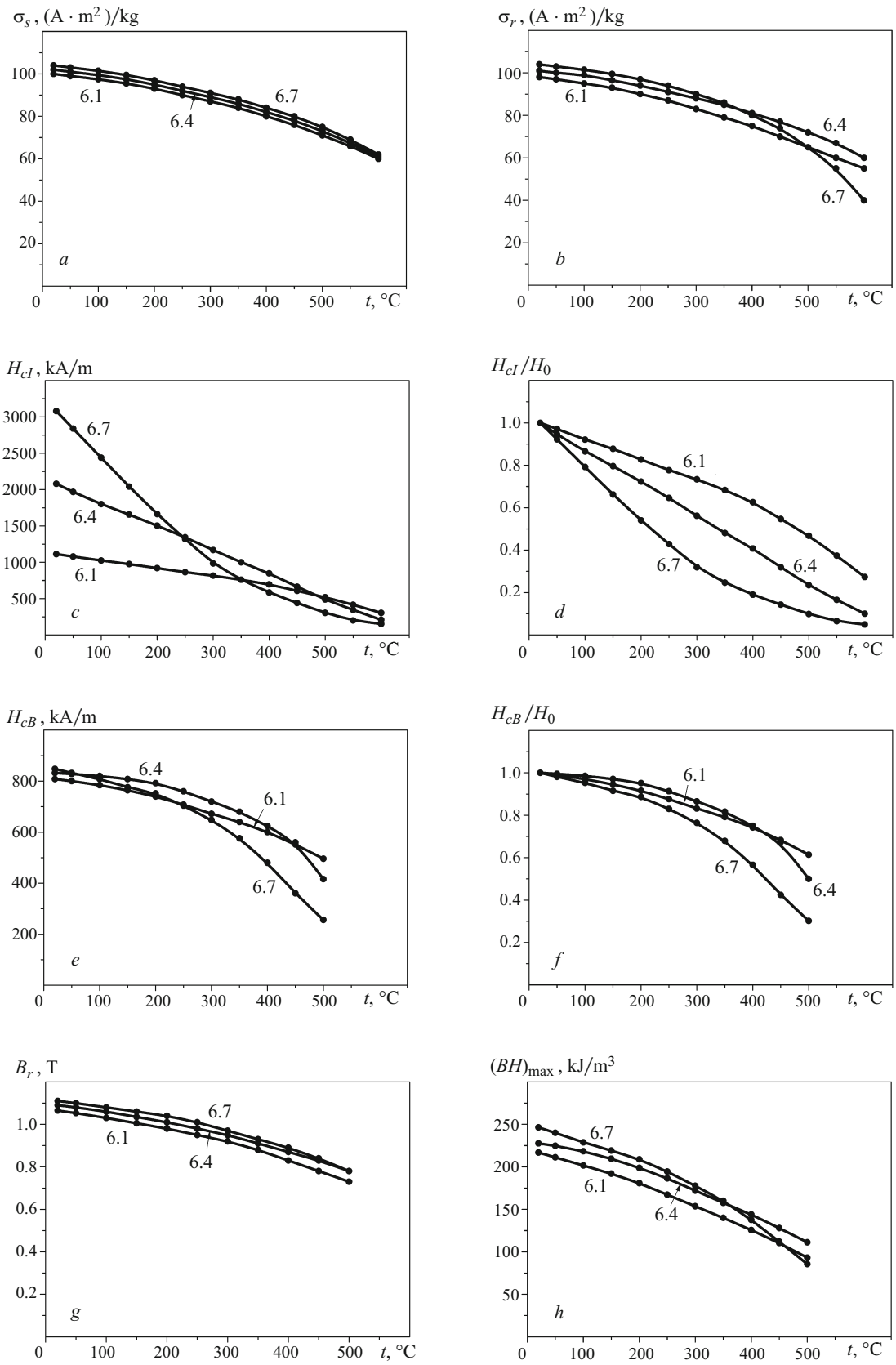

Fig. 2. Temperature dependences of the hysteresis characteristics of alloys $Sm_{0.85}Zr_{0.15}(Co_{0.70}Cu_{0.09}Fe_{0.21})_z$ (the stoichiometric ratio is given at the curves): σ_s) specific saturation magnetization; σ_r) specific residual magnetization; H_{cI} and H_{cB}) magnetization and induction coercivity, respectively; H_{cI}/H_0 and H_{cB}/H_0) reduced dependences (H_0 is the coercivity at 20°C); B_r) residual magnetization; $(BH)_{max}$) maximum energy product.

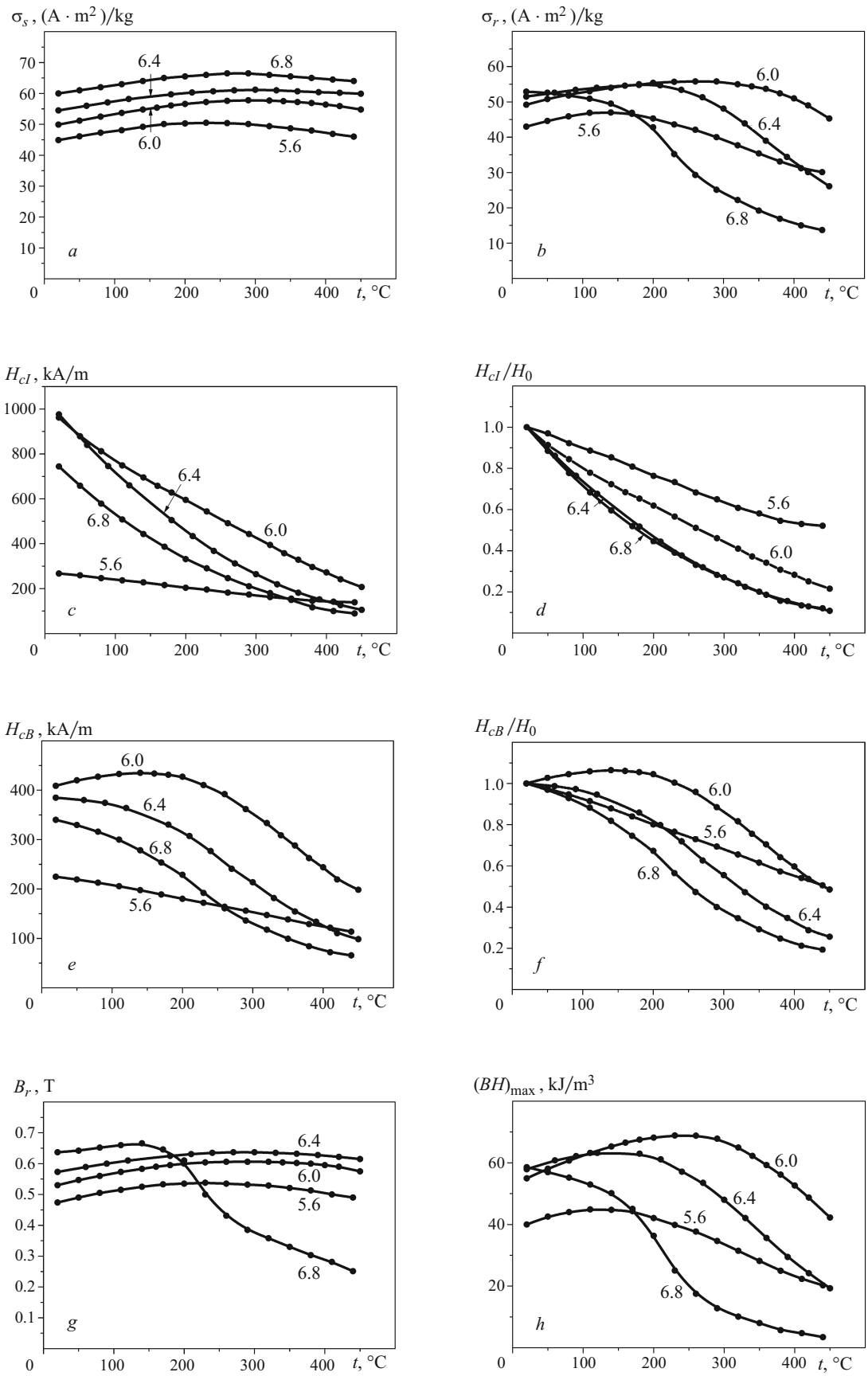

Fig. 3. Temperature dependences of the hysteresis characteristics of alloys $Gd_{0.85}Zr_{0.15}(Co_{0.70}Cu_{0.09}Fe_{0.21})_z$ (the notation is as in Fig. 2).

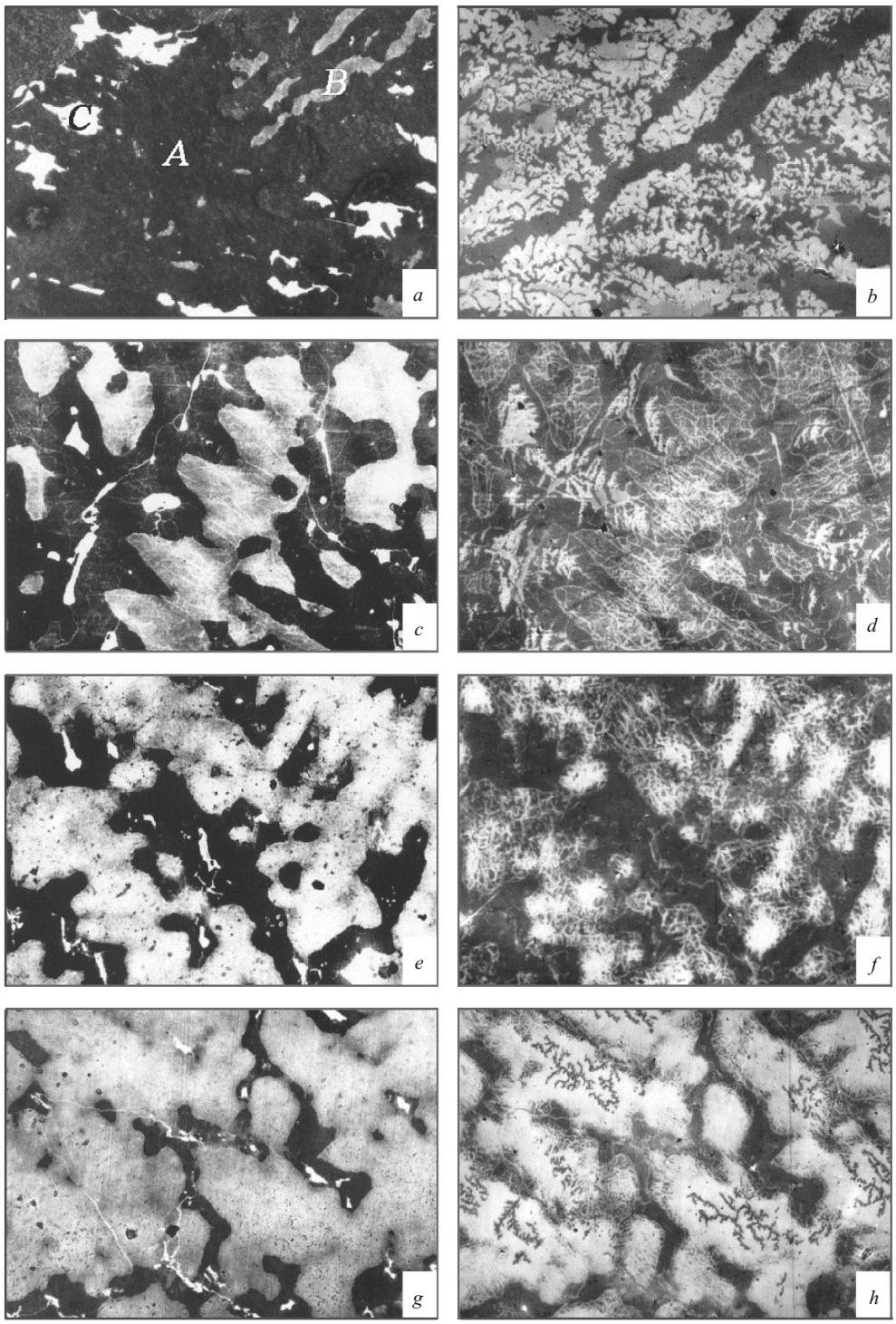

Fig. 4. Microstructure (*a*, *c*, *e*, *g*) and domain structure (*b*, *d*, *f*, *h*) on the base plane of specimens of $Gd_{0.85}Zr_{0.15}(Co_{0.70}Cu_{0.09}Fe_{0.21})_z$ (the size of the circle is 300 × 400 μm).

demagnetizing field with intensity close to the coercive force.

Despite the closeness of the nanostructures of components *A* and *B* (Fig. 5), the configurations of their domain structures differ in principle (Fig. 4). It has been shown in [5, 6] that decrease in the demagnetizing field gives rise to nonequilibrium "pteridophyte" domains in component *A*, and the volume of component *B* is filled progressively with a net of thin wavy domains the width of which virtually does not grow.

It can be seen from Fig. 4*a* and *b* that the demagnetization of the specimen with $z = 5.6$ from saturation to $H_{cI} \approx 240$ kA/m is a result of rearrangement of the domain structure only in component *A*. In the regions occupied with component *B* a domain structure is absent and they remain magnetized to saturation.

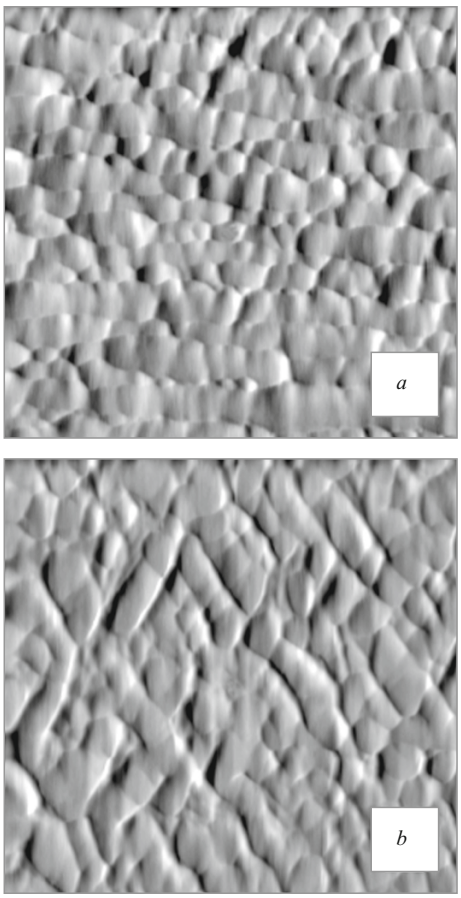

Fig. 5. Typical AFM-images of the surface of structural components *A* (*a*) and *B* (*b*) of alloys (R, Zr)(Co, Cu, Fe) (the scan size is 1 × 1 μm).

Two structural components *A* and *B* participate in demagnetization of the specimen with $z = 6.0$ from saturation to a coercive field $H_{cI} \approx 960$ kA/m; a net of thin domains develops in component *B* and nonequilibrium "pteridophyte"-shaped domains develop in component *A* (Fig. 4*c* and *d*).

Figure 4*e* – *h* show that component *A* remains fully magnetized in the specimens with $z = 6.4$ ($H_{cI} \approx 960$ kA/m) and $z = 6.8$ ($H_{cI} \approx 800$ kA/m), i.e., the process of demagnetization occurs only in component *B*. This explains the virtually similar temperature behavior of the $H_{cI}/H_0(t)$ curves for the specimens with $z = 6.4$ and 6.8 (Fig. 3*d*).

The results obtained in [2, 11] show that similar laws of rearrangement of the domain structure of components *A* and *B* are also typical for specimens of $Sm_{0.85}Zr_{0.15}(Co_{0.70}Cu_{0.09}Fe_{0.21})_z$.

CONCLUSIONS

Our studies of the hysteresis characteristics of magnets and of their structure show an important rule. Alloys $R_{0.85}Zr_{0.15}(Co_{0.70}Cu_{0.09}Fe_{0.21})_z$ with samarium and with gadolinium exhibit lower stability of the coercivity at lower values of *z*. The dominant part of the structure of such alloys is taken by component *A*, which has a stoichiometric ratio $z \approx 5 – 6$ and is enriched with copper as compared to the average composition. This rule should be taken into account when choosing compositions for novel alloys with high temperature stability of the coercivity.

REFERENCES

1. A. E. Ray, "Metallurgical behavior of Sm(Co, Fe, Cu, Zr)$_z$ alloys," *J. Appl. Phys.*, **55**(6), 2094 – 2096.
2. N. P. Suponev, E. B. Shamorikova, A. G. Dormidontov, et al., "Structure and magnetic properties of Sm – Zr – Co – Cu – Fe alloys in highly coercive state. 1. Structural components and processes of magnetization reversal," in: *Intercollege Coll. Papers "Phyz. Magn. Mater."* [in Russian], Kalinin (1988), pp. 93 – 105.
3. N. P. Suponev, A. G. Dormidontov, and V. V. Levandovskii, "Structure and magnetic properties of Sm – Zr – Co – Cu – Fe alloys in highly coercive state. 2. Model of structure formation," in: *Intercollege Coll. Papers "Phyz. Magn. Mater."* [in Russian], Tver (1992), pp. 78 – 98.
4. W. Tang, Y. Zhang, and G. C. Hadjipanayis, "A high performance magnetic alloy with an operating temperature of 500°C," *IEEE Trans. Magn.*, **36**(5), 3294 – 3296 (2000).
5. M. B. Lyakhova, Yu. E. Pushkar, E. B. Shamorikova, et al., "Magnetic properties, phase composition and domain structure of Gd – Zr – Co – Cu – Fe alloys," in: *Intercollege Coll. Papers "Phyz. Magn. Mater."* [in Russian], Kalinin (1985), pp. 90 – 105.
6. Yu. E. Pushkar, M. B. Lyakhova, Yu. V. Babushkin, "Effect of complex alloying on the microstructure and magnetic properties of single crystals based on $GdCo_5$ and Gd_2Co_{17} intermetallic compounds," *Vysokochist. Veshchestva*, No. 4, 164 – 169 (1988).
7. N. P. Suponev, R. M. Grechishkin, M. B. Lyakhova, and Yu. E. Pushkar, "Angular dependence of coercive field in (Sm, Zr)(Co, Cu, Fe)$_z$ alloys," *J. Magn. Magn. Mater.*, **157 – 158**, 376 – 377 (1996).
8. Yu. E. Pushkar and M. B. Lyakhova, "Effect of heat treatments on formation of highly coercive state in Gd – Zr – Co – Cu – Fe alloys," in: *Intercollege Coll Papers "Phyz. Magn. Mater."* [in Russian], Kalinin (1987), pp. 118 – 125.
9. Yu. G. Pastushenkov, N. P. Suponev, M. B. Lyakhova, et al., "A study of the microstructure and domain structure of Sm – Zr – Co – Cu – Fe alloys by methods of optical and atomic-force microscopy," in: *Mining Informative-Analytical Bulletin. Functional Metallic Materials. Raw Materials Base, Magnetic Materials and Systems* [in Russian], MGU, Moscow (2007), Spets. Issue 1, pp. 414 – 426.
10. G. Fidler, P. Scalicky, and F. Rothwarf, "High resolution electron study of Sm(Co, Fe, Cu, Zr)$_{7.5}$ magnets," *IEEE Trans. Magn.*, **MAG-19**(5), 2041 – 2043 (1983).
11. N. P. Suponev, E. M. Semenova, M. B. Lyakhova, et al., "Structure and magnetic properties of nanostructured multicomponent alloys based on 3d- and 4f-metals," *Fiz. Khim. Obrab. Mater.*, No. 3, 48 – 53 (2011).